METHANE/OXYGEN LASER IGNITION IN AN EXPERIMENTAL ROCKET COMBUSTION CHAMBER: IMPACT OF MIXING AND IGNITION POSITION

Michael Wohlhüter, Victor P. Zhukov, Michael Börner

Institute of Space Propulsion, German Aerospace Center (DLR), Langer Grund, 74239 Hardthausen, Germany

Michael.Wohlhueter@dlr.de

KEYWORDS: methane, laser ignition, rocket combustion, GOx/GCH_4, CFD

ABSTRACT: The laser ignition of a GOx/GCH_4 rocket combustion chamber is investigated experimentally and numerically to study the effects of the cold flow conditions on the ignition process. The flame development examined in three laser ignition tests with two different experimental thrusters is compared to the flow conditions and the fluid composition in the combustion chamber obtained in the corresponding CFD simulations. From the results a procedure to achieve smooth ignition is suggested. A short cold flow with fuel rich conditions together with an ignition position downstream of the faceplate is beneficial for a smooth ignition.

1. INTRODUCTION

In recent years the potential use of methane as rocket propellant has received increasing interest worldwide. For upper stage engines and long duration scientific missions, methane can provide beneficial properties compared to the commonly used fuels. The reliable ignition at space conditions is particularly crucial for these types of missions. Thus, detailed knowledge about the flame behavior in methane/oxygen mixtures in rocket combustion chambers at low initial pressures is required.

At the DLR Institute of Space Propulsion several experimental [1,2,3] and numerical [4,5,6] investigations of laser ignition in experimental combustion chambers were realized. Recent work [6] shows flame front acceleration during the spreading of the flame in the combustion chamber, leading to strong pressure peaks, so called hard ignitions.

Goal of the present work is the study of the origin of this behavior and, by combining experimental and numerical investigations, to identify the impact of mixing and ignition position on the flame development during ignition.

Especially regarding rocket combustion chambers, numerical simulations can provide important insight into the situation and phenomena occurring in the combustion chamber, where measurement access is very limited. While in experiments quantitative data is mainly restricted to pressure and temperature measurement at selected points, simulations can provide data of the flow field as well as the species and temperature distribution.

The ignition test can be divided in two phases. The first phase before the laser pulse is the filling of the combustion chamber with propellants and the second phase is the ignition and subsequent combustion of the propellants. In the first phase the main aspect is the injection and mixing of the propellants and their distribution within the combustion chamber. The amount and distribution of the fuels is directly connected to flame spreading and the pressure peak occurring during ignition. The second phase covers the laser pulse and subsequent flame development throughout the combustion chamber.

This conference paper reports on the conditions in the combustion chamber at the time of ignition and their impact on the flame development. The goal is to improve the understanding of the ignition processes, to be able to choose better cold flow conditions and ignition positions to avoid high ignition pressure peaks.

2. EXPERIMENTAL SETUP

For the experimental investigations providing the data used in the present work, two versions of a 400 N experimental thruster together with a tabletop laser ignition system were used. The sections below further describe the thrusters, the laser ignition system and the measurement systems. More detailed information about the experimental setup can be found in [3,5].

Three test cases are compared to get more insight into the flame development under different conditions. Table 1 shows an overview over the

test cases and their settings for ignition position, the valve opening times and the mass flows of the propellants. Test case A is the RCSLaser test case used in [6]. For the investigations in this paper it is compared with two test cases of the MOLI (Methane/Oxygen Laser Ignition) experiments, named test case B and C. Test case B has similar cold flow conditions to test case A, but lower mass flows of the propellants. It also shows a hard ignition with a strong pressure peak. For test case C, the second MOLI test, the main goal was to achieve a smooth ignition with low pressure peak by shortening the cold flow before ignition and changing the opening sequence of the valves.

2.1. The combustion chambers

Experimental data from tests with two different combustion chamber geometries are used in the present work. The cross sections of the combustion chambers are shown in Fig. 1. The 60 mm-diameter cylindrical section is the same for both combustion chambers, which allows the use of the same injector and window configuration as well as the same sensor positions. A single coaxial injector element without recess and tapering is used to inject the propellants into the combustion chamber. Quartz windows in the side walls provide optical access for the optical diagnostics systems, the laser enters through a small window at the top of the chamber. The main difference between the two combustion chambers is the nozzle throat diameter. The RCSLaser chamber has a throat diameter of d_{th} = 32 mm. To gain a pressure increase in this combustion chamber during the test, high mass flows of the propellants had to be chosen. High injection velocities resulted, which could influence the ignition process. To get information at different test conditions the MOLI combustion chamber was designed with a significantly smaller throat diameter of d_{th} = 10 mm. In these tests lower mass flows could be used, which resulted in lower injection velocities.

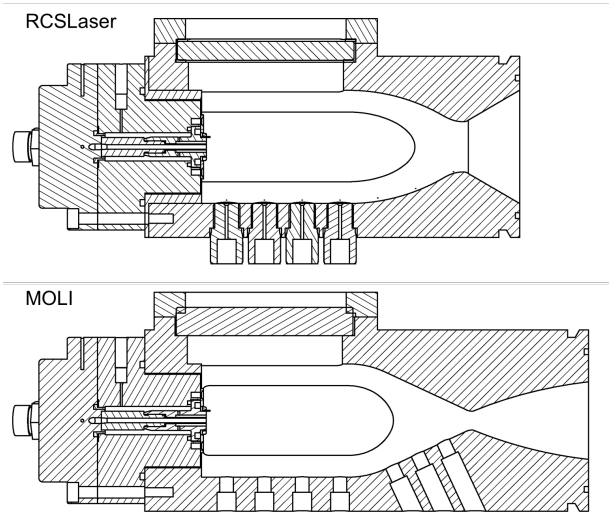

Figure 1: RCSLaser and MOLI thruster cross section

2.2. The laser ignition system

A frequency doubled Nd:YAG laser with a wavelength of 532 nm was used to deliver the laser pulse for ignition. The power of the laser pulse was in range of 90 mJ. The laser beam was

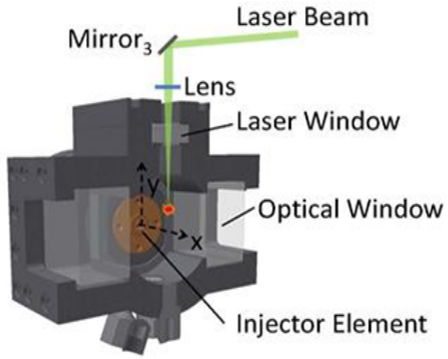

Figure 2: Laser pulse path into the combustion chamber [3]

Table 1: Test case overview

Test case	Combustion chamber	Nozzle throat diameter [mm]	Ignition position [mm]		Valve opening time [ms]		Mass flow [g/s]	
			X	Y	CH_4	O_2	CH_4	O_2
A	RCSLaser	32	2	7	-7	-82.5	12	37
B	MOLI	10	4	6	-14	-77	3	9
C	MOLI	10	4	2	-33	-31	4	12.5

focused into the combustion chamber via a lens through the small top window, as shown in Fig. 2. The focus point of the laser for all tests used in this work was close to the face plate. The exact positions relative to the face plate and central axis can be found in Tab. 1.

2.3. Measurement systems

The combustion chambers are equipped with four piezoelectric and four piezoresistive absolute pressure sensors along the lower cylindrical section. These sensors were used to measure the ignition pressure peaks and the steady state chamber pressure, respectively. The piezoelectric pressure sensors are faster, but temperature sensitive, so they are used in the early stages of the ignition. The piezoresistive pressure sensors are slower, but not temperature sensitive. They are used to measure the pressure in the later stages of the test. Both types of pressure sensor are also installed in the injector head to measure the pressure of the propellants in each respective injector dome.

Temperature is measured in the injector domes to define the injection conditions of the propellants.

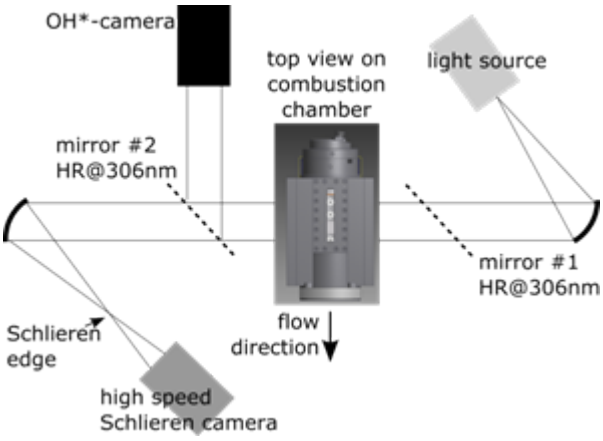

Figure 3: Optical diagnostics setup [7]

To gather information about the flow conditions and the flame development in the combustion chamber, the test bench is equipped with Schlieren- and OH*-/CH* emission optical diagnostics systems. A standard Z-setup, as shown in Fig. 3 , is used for Schlieren imaging. Spontaneous OH*/CH*-emission is recorded by an intensified high-speed CCD camera.

3. NUMERICAL SETUP

The simulations were done with the commercial Computational Fluid Dynamics (CFD) solver ANSYS CFX, version 14.5 [8]. The Shear Stress Turbulence (SST)-model of Menter [9] was used in the URANS (Unsteady Reynolds-Averaged Navier-Stokes) calculations presented in this paper.

3.1. Geometry and mesh

The computational domain used in the simulations is composed by three parts:

- Coaxial injector with central oxygen post and surrounding methane annulus
- Combustion chamber with exit nozzle
- Ambient area, into which the combustion gases expand

The combustion chamber and the injector geometry have no common symmetry plane. Thus, only simulations taking into account the full 3D geometry can produce all effects caused by the flow. Previous investigations have shown that simplifications made to reduce the mesh size, such as reorientation of the injector to match the symmetry planes and model a 180°-geometry, influence the distribution of propellants in the combustion chamber and thus the ignition process [5]. Figure 4 shows the geometry of the combustion chambers and the injector geometry in their appropriate orientation.

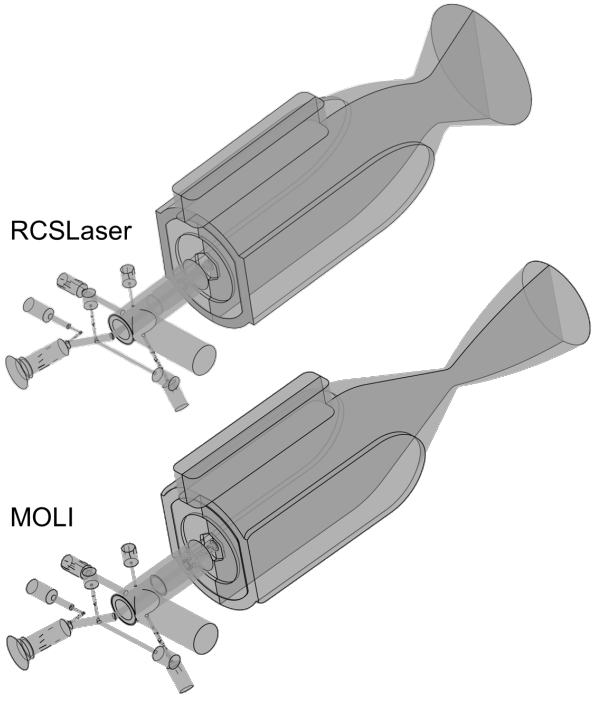

Figure 4: Combustion chamber and injector geometries of RCSLaser and MOLI simulations

The injector mesh consists of 150k nodes. The combustion chamber is meshed with 1.2 Mio nodes for the RCSLaser simulations and with 1.3 Mio nodes for the MOLI simulations.

3.2. Initialization and boundary conditions

Preceding each test, the combustion chamber is purged with nitrogen to ensure defined start conditions. Hence, as initial condition of the simulation the combustion chamber and the injector are completely filled with quiescent nitrogen at ambient conditions. The ambient area is defined as air at ambient conditions. The simulation starts with the opening of the first run valve and models the pressure rise in the injector domes and the filling of the combustion chamber with propellants. The energy input of the laser pulse is modeled and the flame development with the pressure peak following the laser ignition are simulated, followed by the relaxation of the combustion chamber pressure to the steady state value.

All walls of the injector geometry are treated as adiabatic walls, in the combustion chamber they are defined as isothermal walls at ambient temperature. During ignition this is a valid assumption, as there is not enough time for the flame to heat up the walls. No-slip conditions are applied to all walls.
At the outlet boundary of the ambient area opening boundary conditions are applied with ambient pressure and temperature.

Pressure is specified as inlet conditions for both the oxygen and methane inlet to achieve the proper mass flow development in time with changing combustion chamber pressure. Methane and oxygen both have the temperature of T = 278 K. The simulations have different cold flow sequences. The opening times of the run valves are set in Tab. 1 as well as the mass flow values at steady flow to show the different conditions. The time of ignition is set as zero.

4. RESULTS AND DISCUSSION

Three test cases are compared to get more insight into the flame development under different conditions. Test case A is the RCSLaser test case used in [6]. This test case is compared with two test cases with the MOLI combustion chamber, as shown in Tab. 1.

This section will take a look at the differences and similarities of the three tests. To identify some of the main processes leading to hard or soft ignitions, both experimental and numerical results are used. First the flame development following the laser pulse is considered. This part concentrates on experimental data of the optical diagnostics systems. In further steps those observations are compared to the flow conditions and the species distribution in the combustion chamber at the time of ignition. Numerical results are used for these investigations, as no experimental data regarding these values are available.

4.1. Flame development

The flame development following the laser pulse defines the heat release and the pressure evolution in the combustion chamber. Information about the flame development is gained by the optical diagnostics systems used in the experimental investigations. Figure 5 shows Schlieren image sequences of the flame development in the three test cases. While the

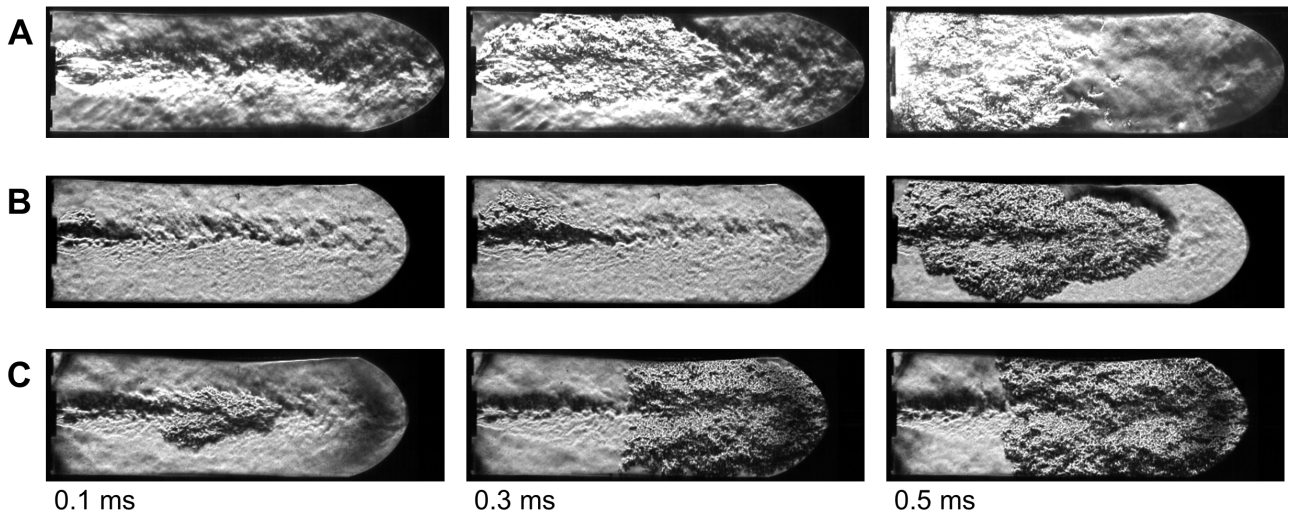

Figure 5: Flame development in the test cases

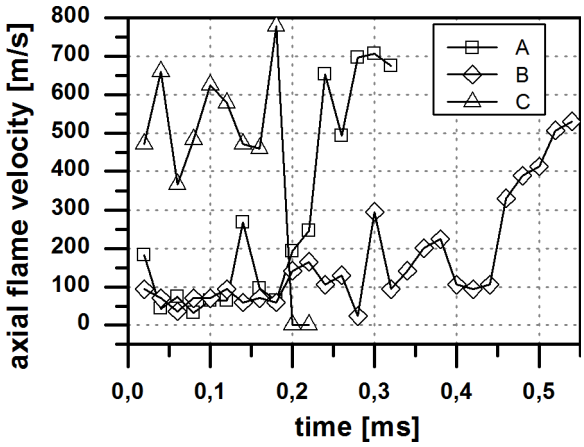

Figure 6: Evolution of axial flame velocities

flame is progressing through the combustion chamber, the flame front is visible in the Schlieren images by the density gradients between cold gases in front of and hot gases behind the flame front.

As described in [6], in test case A in the beginning the flame spreads with constant flame velocity in axial direction, but at a certain time the flame front accelerates up to supersonic speeds. This leads to a strong pressure rise in the combustion chamber. The evolution of the axial velocity of the downstream flame front for all three test cases is shown in Fig. 6. These values were derived from the experiments by measuring the frame to frame progression of the downstream flame front in the Schlieren images.

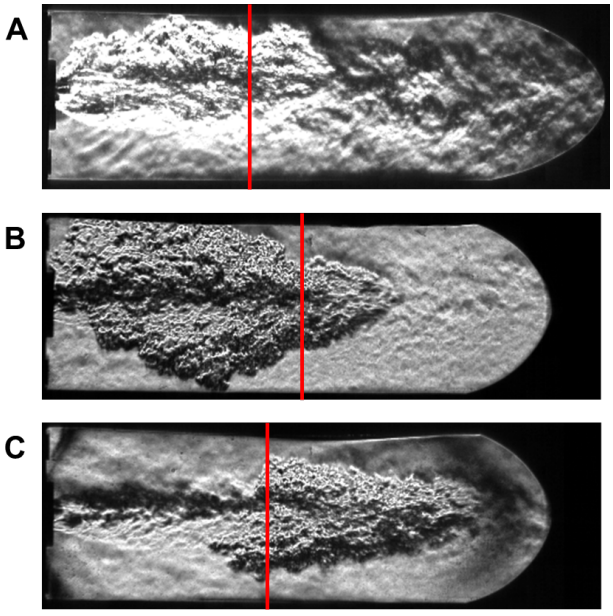

Figure 7: Transition of flame state in test cases

Test case B has similar cold flow conditions to test case A, in spite of significantly lower mass flow rates and injection velocities of the propellants. Although the time frame is different, the general behavior of the flame is similar for the test cases A and B. In the early stages after the laser pulse the flame speed remains constant at about 75 m/s, before after 0.2 ms the downstream flame front accelerates towards supersonic speeds up to 700 m/s.

Test case C shows a significantly different flame development than the other two tests. In the early stages the flame mainly spreads in the shear layer of the main flow in axial direction driven by the flow, without growing in the radial direction on a larger scale. At an axial distance of 38 mm from the faceplate the transition occurs and the flame starts to grow in radial direction as well. The upstream flame front stays at this axial position, until the hot gases from the downstream flame move back upstream in the recirculation zones.

Table 2: Axial value of transition point

Test case	X [mm]
A	34
B	46
C	38

Figure 7 shows Schlieren images of the three test cases, where the transition of the flame state is visible. The axial transition position is marked by the red lines. Although the three tests differ in combustion chamber geometry, cold flow conditions and mass flow settings, the axial position of the transition to flame front acceleration and large scale expansion of the flame respectively is very similar for all of them, as shown in Tab. 3.

4.2. Species distribution

One main influencing factor for the ignition process is the amount and distribution of propellants in the combustion chamber at the time of ignition. As the experiments do not provide data about these properties, numerical simulations allow insights into the situation in the combustion chamber at the

time of ignition. In Tab. 3 the global mass fractions of CH_4, O_2 and N_2 are presented for the three tests, averaged by the combustion chamber volume. The Ratio Oxidizer-to-Fuel (ROF) by mass is calculated as well to give an idea about the overall mixture condition in the combustion chamber. The stoichiometric value of CH_4/O_2-mixtures is ROF = 4. Higher values mark lean mixtures with excess of O_2, lower values mark rich mixtures with an excess of CH_4.

For the test cases A and B, the overall conditions at the time of ignition are very similar. The ROF is high in both cases, meaning the mixture is O_2-rich. The CH_4 mass fraction is low due to the opening of the run valve only short before ignition. One difference is the N_2 mass fraction. While in test case A only a low amount of N_2 is still present at the time of ignition, test case B still shows a N_2 mass fraction of 0.288. The mixture here is much more diluted. At test case C the overall situation at time of ignition is different. The amount of CH_4 is four times higher than in the other tests, while the amount of O_2 is less. This leads to a rich mixture with an excess of CH_4 and a ROF of 2.2. Also the N_2 mass fraction is the highest of the three tests,

Table 3: Main species mass fractions in the combustion chamber at the time of ignition

Test case	Mass fraction CH_4	Mass fraction O_2	Mass fraction N_2	Global ROF
A	0.043	0.936	0.020	21.8
B	0.035	0.677	0.288	19.2
C	0.194	0.426	0.379	2.2

as because of the short cold flow there is only few time to flush out the N_2 before ignition takes place. The Figures from 8 to 11 show the distribution of propellants on the central xy-plane in the combustion chamber at the time of ignition.

The contour plots of the ROF distribution in Fig. 8 capture ROF-values between zero and eight. Values higher than eight are clipped and shown in bright green color, as otherwise the ROF range closer to the stoichiometric value $ROF_{st} = 4$ and lower is not visible. The test cases A and B show a quite similar situation. The stoichiometric mixtures in these tests are near the CH_4 main flow, while in the recirculation zone a O_2-rich mixture is present. Test case C shows a very different situation. The mixture in the recirculation zone is rich. Near the faceplate stoichiometric mixtures are present only in the shear layer between CH_4 and O_2. Further downstream near stoichiometric mixtures exist in a bigger region when the O_2 main flow mixes with the surrounding fluid.

The CH_4 distribution in the combustion chamber, as seen in Fig. 9, shows a similar behavior. The test cases A and B have significant amounts of CH_4 only in the main flow near the injector. Further downstream and in the recirculation zone only low amounts of CH_4 are present. At test case C a high amount of CH_4 is present in all regions of the combustion chamber.

The O_2 distribution for all three tests at the time of ignition is shown in Fig. 10. At test case A the combustion chamber is almost completely filled with O_2. The CH_4 flow mixes with the O_2, so in the downstream region of the combustion chamber the amount of O_2 is slightly lower. At test case B the O_2 main flow mixes thoroughly in the downstream part of the combustion chamber and reaches a value of 75 % in the recirculation zones. In test case C the amount of O_2 is lower. The main jet is present in the first part of the combustion chamber, before it mixes with the surrounding fluids.

The biggest difference between the tests is the N_2 distribution. In test case A almost all N_2 is flushed out of the combustion chamber, while in the the test cases B and C residual N_2 from the pre-test purging is still present at the time of ignition. Figure 11 shows that N_2 concentrations are higher near the faceplate, indicating a higher dilution of the propellants.

4.3. Discussion

The Schlieren images show that a transition of flame development occurs at all three tests. At the test cases A and B an acceleration of the flame front velocity is observed up to supersonic velocities. This leads to high pressure peaks, so called hard ignitions. Test case C shows a transition of the flame from being confined mainly in the shear layer to an expansion on large scale also radially. All three cases show this transition behavior around an axial distance from the faceplate of x = 40 mm. This distance matches the mixing of the main CH_4 (test case A) and O_2 flow (test cases B and C) with the surrounding fluid in the simulations. In the test cases B and C considerable amounts of N_2 are still present at time

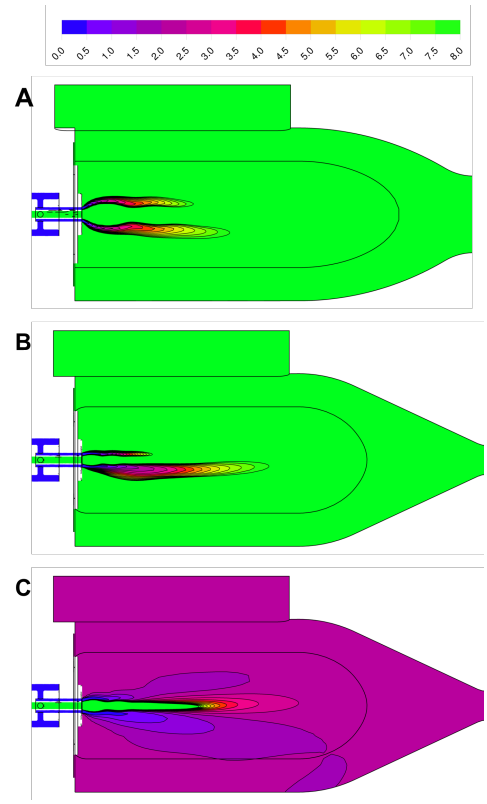

Figure 8: ROF distribution in the combustion chamber at the time of ignition

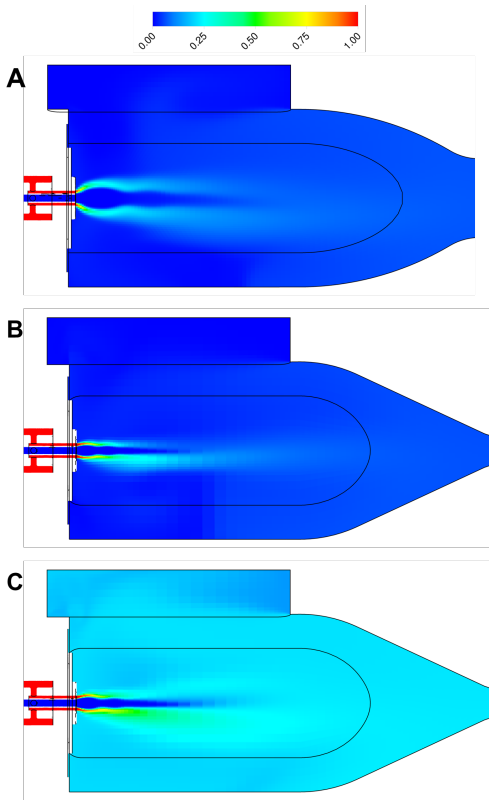

Figure 9: CH_4 distribution in the combustion chamber at the time of ignition

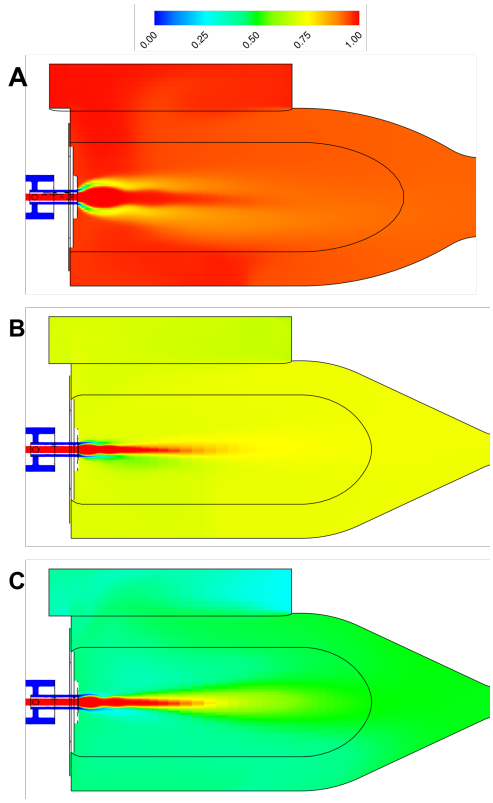

Figure 10: O_2 distribution in the combustion chamber at the time of ignition

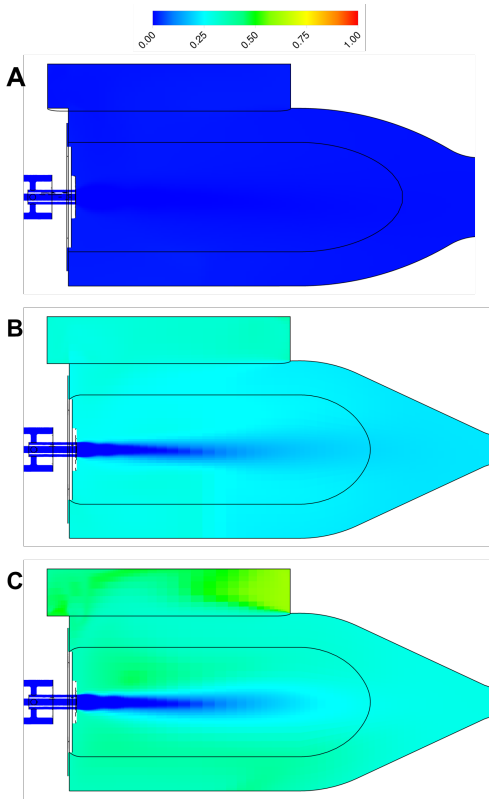

Figure 11: N_2 distribution in the combustion chamber at the time of ignition

of ignition. No significant influence of the N_2 concentration on the flame development has been observed in the tests, as the flame acceleration takes place in test case B as well as in test case A, where only low amounts of N_2 are left in the combustion chamber at time of ignition. The main difference between the hard ignition test cases A and B and the smooth ignition case C is the O_2 concentration, caused by the different cold flow sequences specified in Tab. 1. The test cases A and B had a similar cold flow setup with long O_2 preflow and short CH_4 preflow, while test case C had a short cold flow with equal preflow times for CH_4 and O_2. While the former show lean mixtures with ROF ~ 20 in the combustion chamber, in the latter case a fuel rich mixture with ROF = 2 is present. These observations lead to the conclusion, that a short and fuel rich cold flow is preferable to achieve a smooth ignition. As the propellants need time to mix, an ignition point downstream the faceplate seems beneficial, around or downstream the transition point at x = 40 mm. Considering the use of cryogenic propellants, this aspect gains relevance, because mixing is more difficult and takes more time, as propellants have to be atomized.

5. SUMMARY

Previous investigations with the RCSLaser combustion chamber on CH_4/O_2 laser ignition showed undesirable flame behavior with flame acceleration up to supersonic velocities and hard ignitions. To study the processes leading to hard ignitions tests were done with a new designed combustion chamber with smaller throat diameter. This paper focuses on the flame development observed in these tests and the conditions at the time of ignition, which were obtained by numerical simulations.

In the present work three tests have been compared. Test case A, the RCSLaser test, which showed the hard ignition, was compared to two MOLI tests. Test case B had a similar cold flow setup with long O_2 preflow and short CH_4 preflow, while test case C had a short preflow with equal preflow times for CH_4 and O_2. Test case B showed a hard ignition as well, while case C achieved a smooth ignition with low pressure peak.

The main difference between the tests is the O_2 concentration in the combustion chamber at the time of ignition. While the test cases A and B have high concentrations of O_2, leading to a lean mixture with ROF ~ 20, test case C shows a low concentration of O_2 and a fuel rich mixture with ROF = 2.

In all three tests a transition in the flame development could be observed at a transition point around 40 mm downstream the faceplate. For the test cases A and B from here the flame front starts to accelerate up to supersonic speeds, for test case C the flame starts to spread radially after being confined mainly in the shear layer. This distance matches the mixing of the main CH_4 (test case A) and O_2 flow (test cases B and C) with the surrounding fluid in the simulations, which leads to high amounts of flammable mixture further downstream.

The present study indicates that a short cold flow with fuel rich conditions is favorable to achieve a smooth ignition. For laser ignition the ignition point preferably is located at or downstream of the transition point, as there are better ignition conditions due to the better mixing of the propellants.

6. REFERENCES

1. Pauly, C., Sender, J. & Oschwald, M. (2007). *Ignition of a Gaseous Methane/Oxygen Coaxial Jet*. 2nd European Conference for Aerospace Sciences (EUCASS).

2. Sender, J., Manfletti, C., Oschwald M. & Pauly, C. (2008). *Ignition Transients of a gaseous CH4/O2 coaxial jet*. 22nd European Conference on Liquid Atomization and Spray Systems.

3. Manfletti, C. & Börner, M. (2014). *Ignition Overpressure in Laser Ignited Reaction and Control Thrusters*. 50th AIAA/ASME/SAE/ASEE Joint Propulsion Conference 2014, Cologne.

4. Haidn, O., Palkina, I., Riccius, J. & Gernoth, A. (2007). *Analysis of a Model Combustor Ignition and Comparison with Experimental Results*. 43rd AIAA/ASME/ASEE Joint Propulsion Conference and Exhibit.

5. Wohlhüter, M., Zhukov, V. P. & Manfletti, C. (2014). *Numerical Analysis of Laser Ignition and Flame Development in a Subscale Combustion Chamber*. Space Propulsion Conference 2014, Cologne.

6. Wohlhüter, M. & Zhukov, V.P. (2015). *Numerical analysis of methane/oxygen laser-ignition*. 6th European Conference for Aerospace Sciences (EUCASS).

7. Börner, M. & Manfletti, C. (2014). *Laser Ignition of a multi-injector liquid rocket engine*. Space Propulsion Conference 2014, Cologne.

8. ANSYS CFX, ANSYS® Academic Research, Release 14.5.

9. Menter, F.R. (1994). *Two-Equation Eddy-Viscosity Turbulence Models for Engineering Applications*. AIAA Journal, Vol. 32, No. 8, pp. 1598-1605.

Methane/oxygen laser ignition in an experimental rocket combustion chamber: Impact of mixing and ignition position

Michael Wohlhüter

German Aerospace Center (DLR), Institute of Space Propulsion

Introduction
Hard vs. Smooth ignition

B: Hard ignition

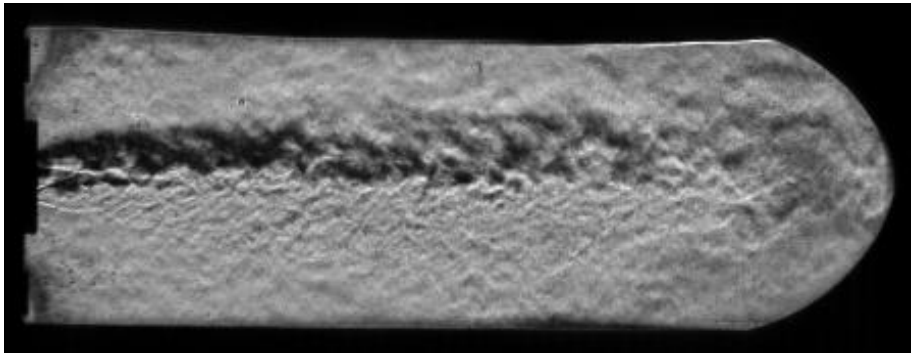

C: Smooth ignition

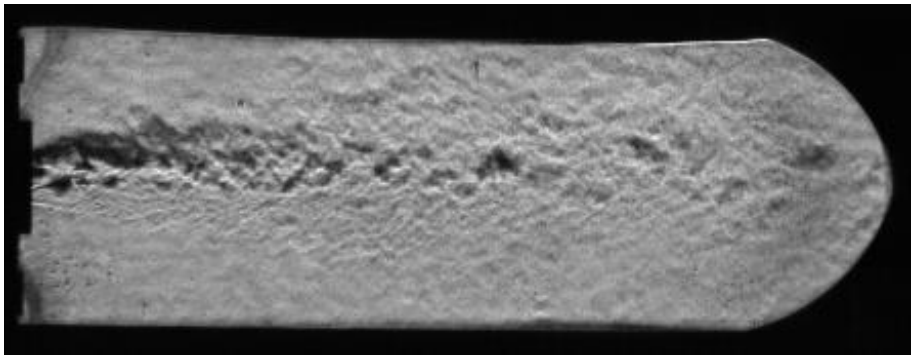

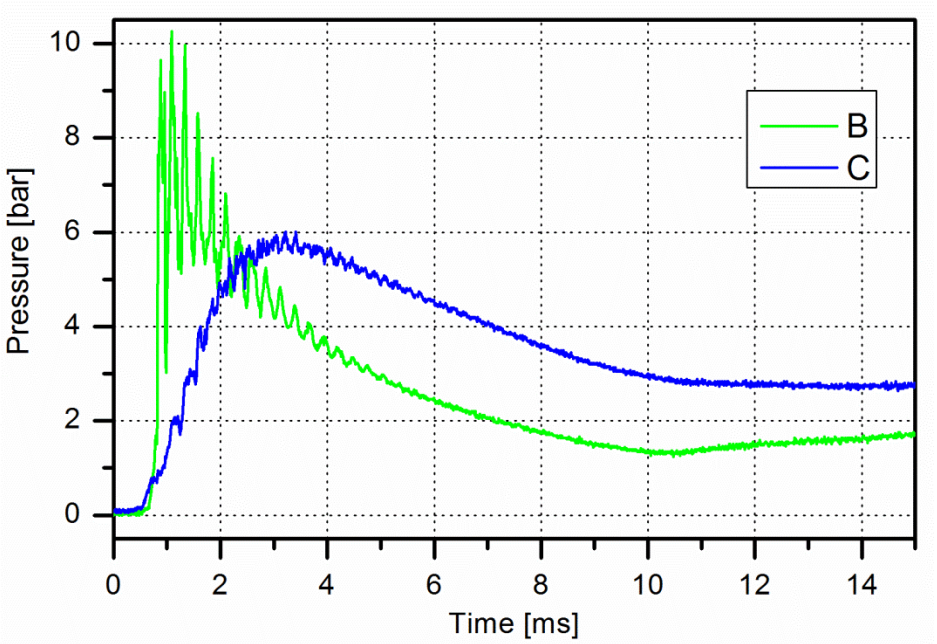

Original time: 5 ms, 50000 fps
Video: 10 s, 25 fps

Review RCSLaser

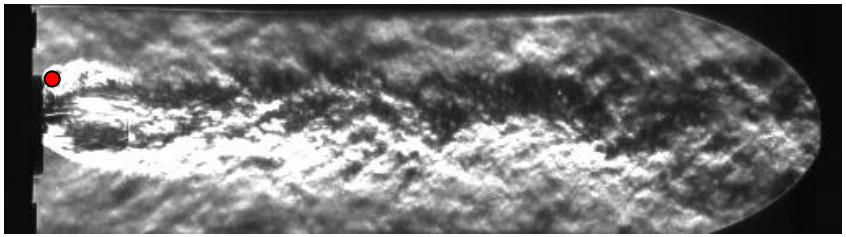

0,12ms

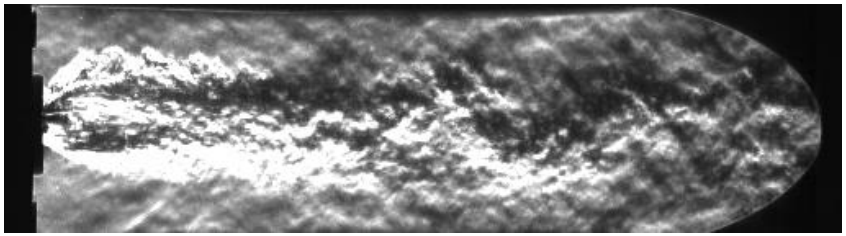

0,22ms

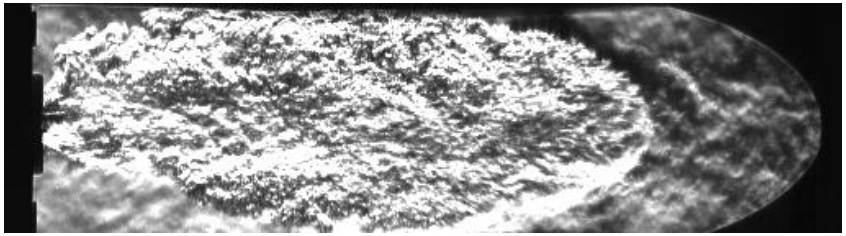

0,32ms

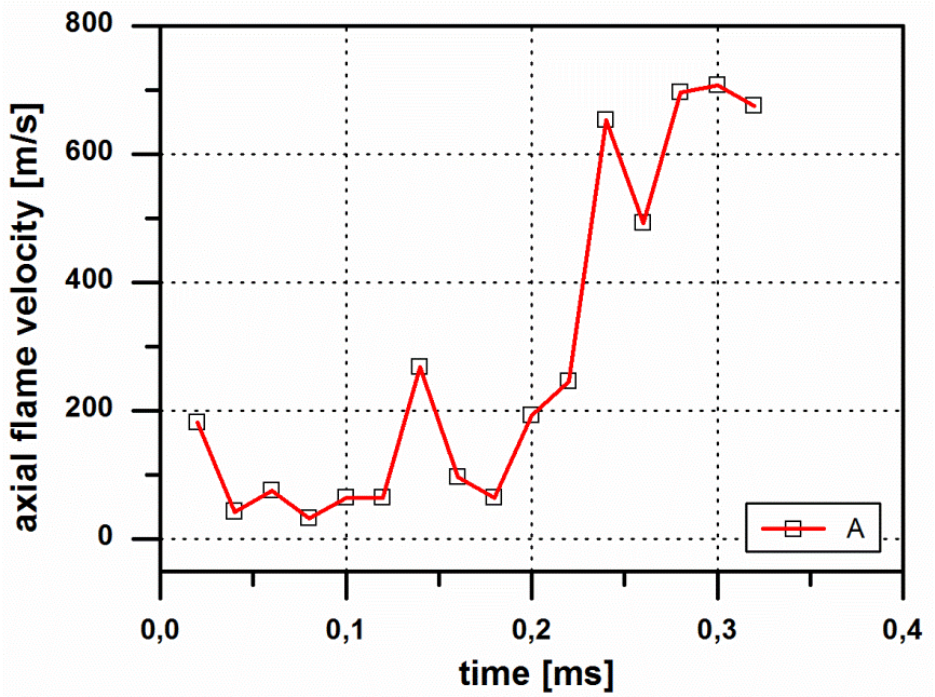

Experimental setup
Combustion chamber

RCSLaser

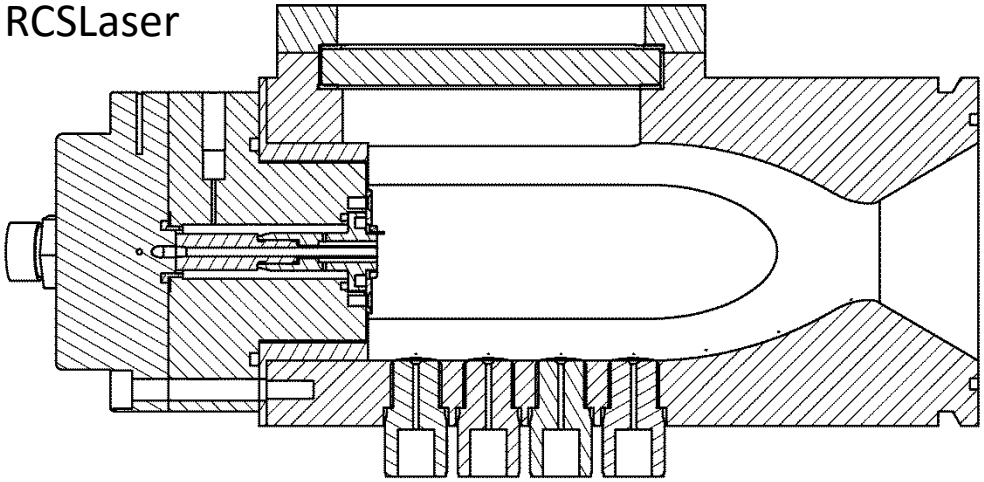

MOLI

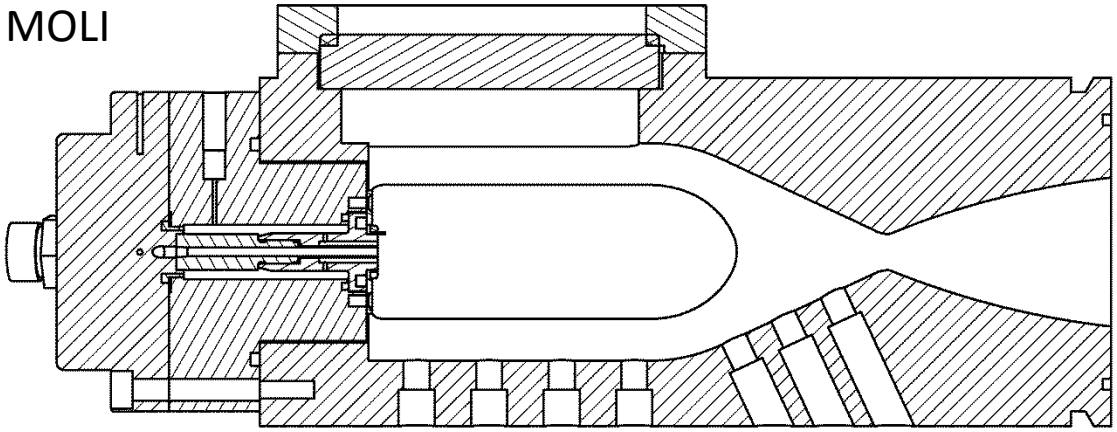

Experimental setup
Test bench and measurement systems

- Combustion chamber:
  - Semicylindrical, diameter d_c=60 mm, length l_c=140 mm
  - Single coaxial injector
- Laser ignition system
  - Frequency doubled Nd:YAG laser, λ=532 nm
  - Pulse length 10 ns, pulse energy ~90 mJ

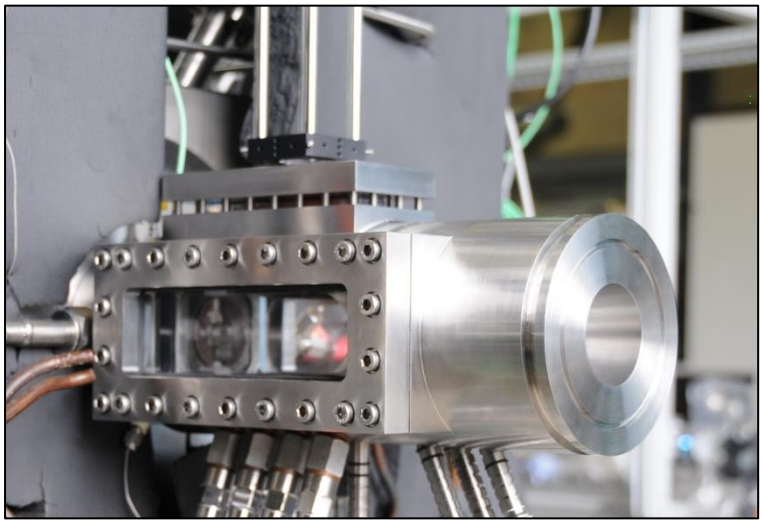

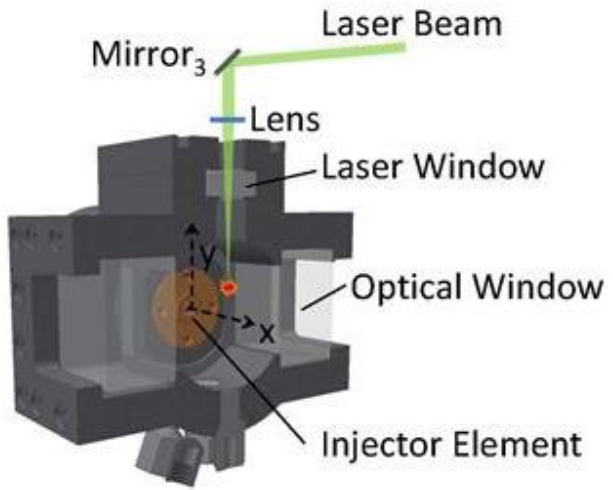

Experimental setup
Test bench and measurement systems

- Combustion chamber:
  - Semicylindrical, diameter d_c=60 mm, length l_c=140 mm
  - Single coaxial injector
- Laser ignition system
  - Frequency doubled Nd:YAG laser, λ=532 nm
  - Pulse length 10 ns, pulse energy ~90 mJ
- Optical diagnostics
  - Schlieren camera
  - OH* camera
- Piezoelectric („dynamic“) and piezoresistive („static“) pressure sensors

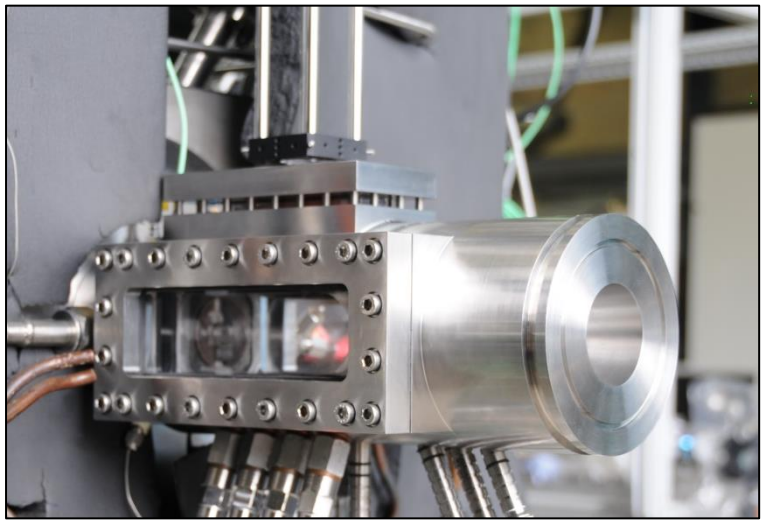

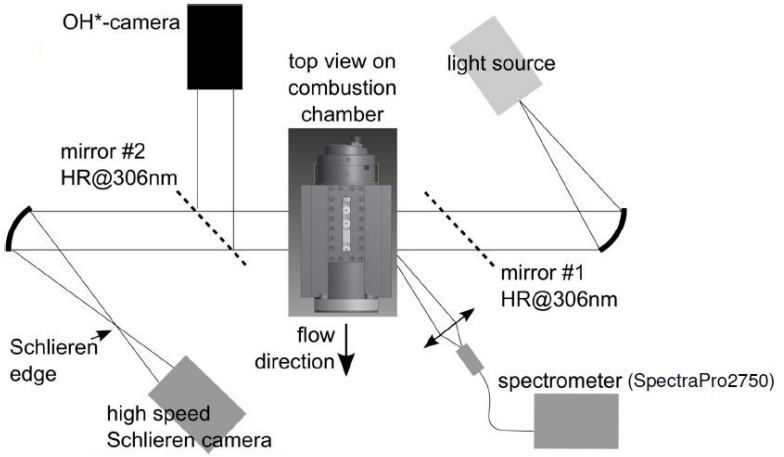

Numerical setup

- ANSYS CFX, Version 14.5
- URANS turbulence model:
  Shear Stress Turbulence (SST)
- Full 3D Mesh:
  - Injector:
    tetraedral mesh with prism layers,
    150 k nodes
  - Combustion chamber:
    hexaedral mesh
    - RCSLaser: 1.2 Mio nodes
    - MOLI: 1.3 Mio nodes

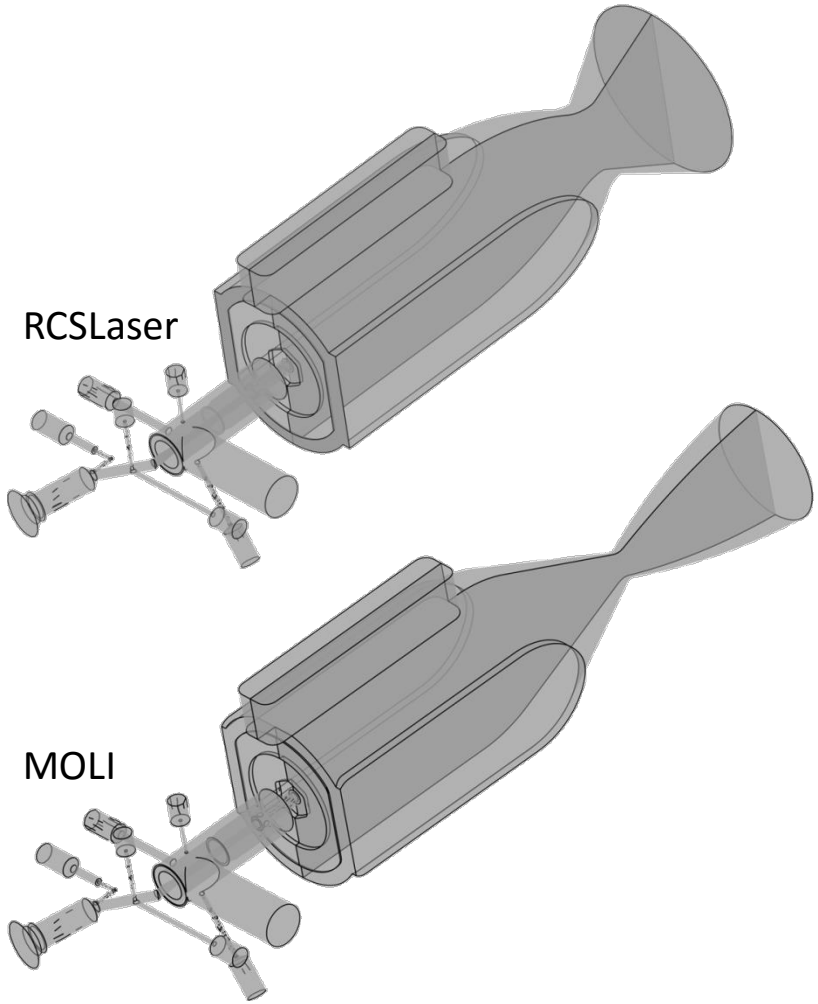

Experimental conditions

Test case	Combustion chamber	Nozzle throat diameter [mm]	Ignition position [mm]		Valve opening time [ms]		Mass flow [g/s]	
			X	Y	CH_4	O_2	CH_4	O_2
A	RCSLaser	32	2	7	-7	-82.5	12	37
B	MOLI	10	4	6	-14	-77	3	9
C	MOLI	10	4	2	-33	-31	4	12.5

Experimental Results
Flame development

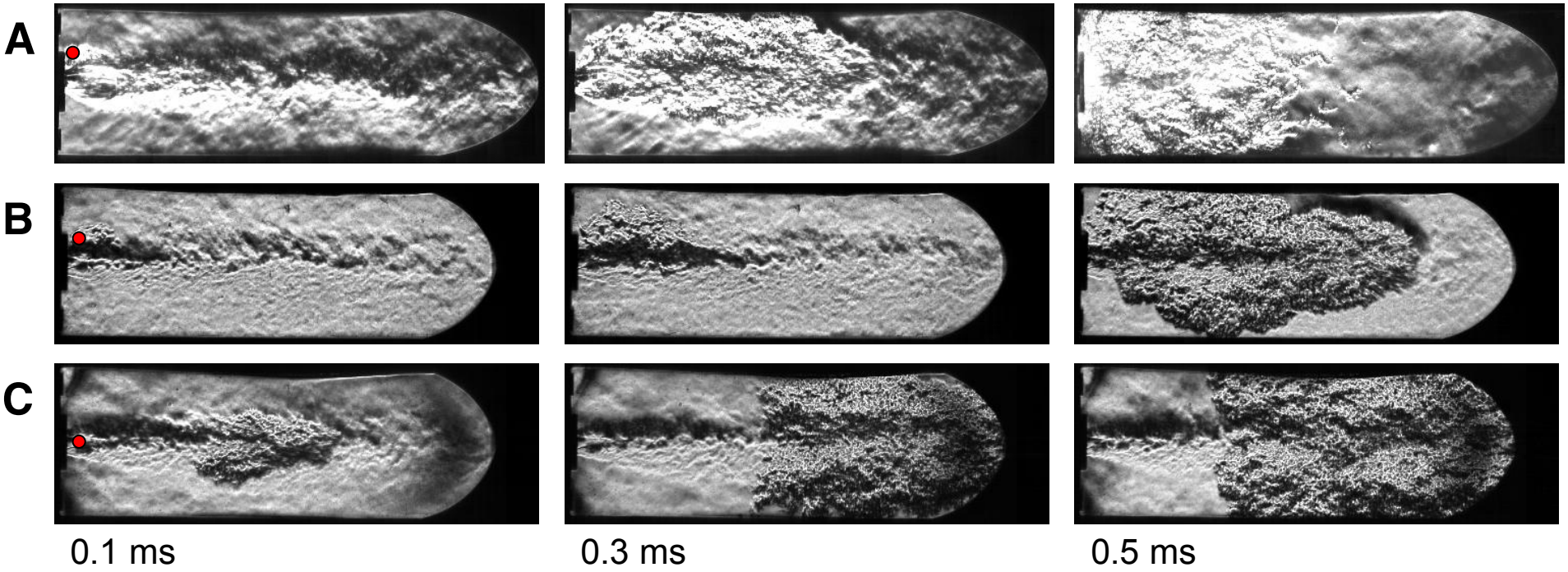

Experimental Results
Flame development

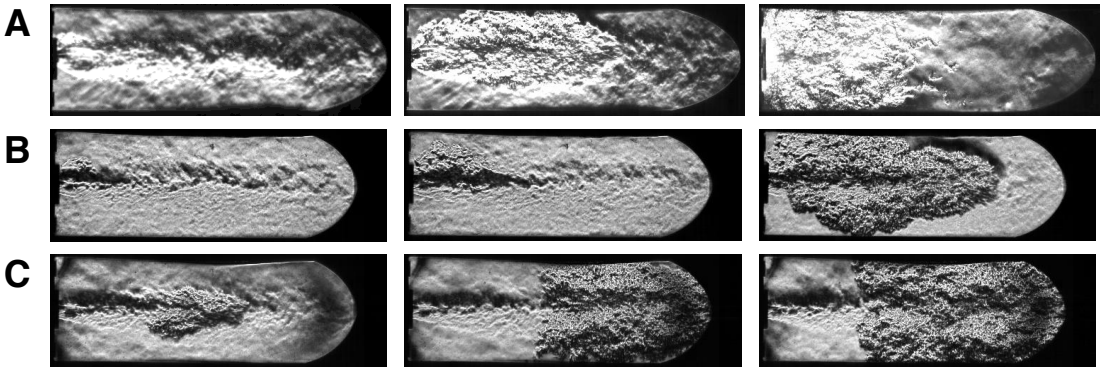

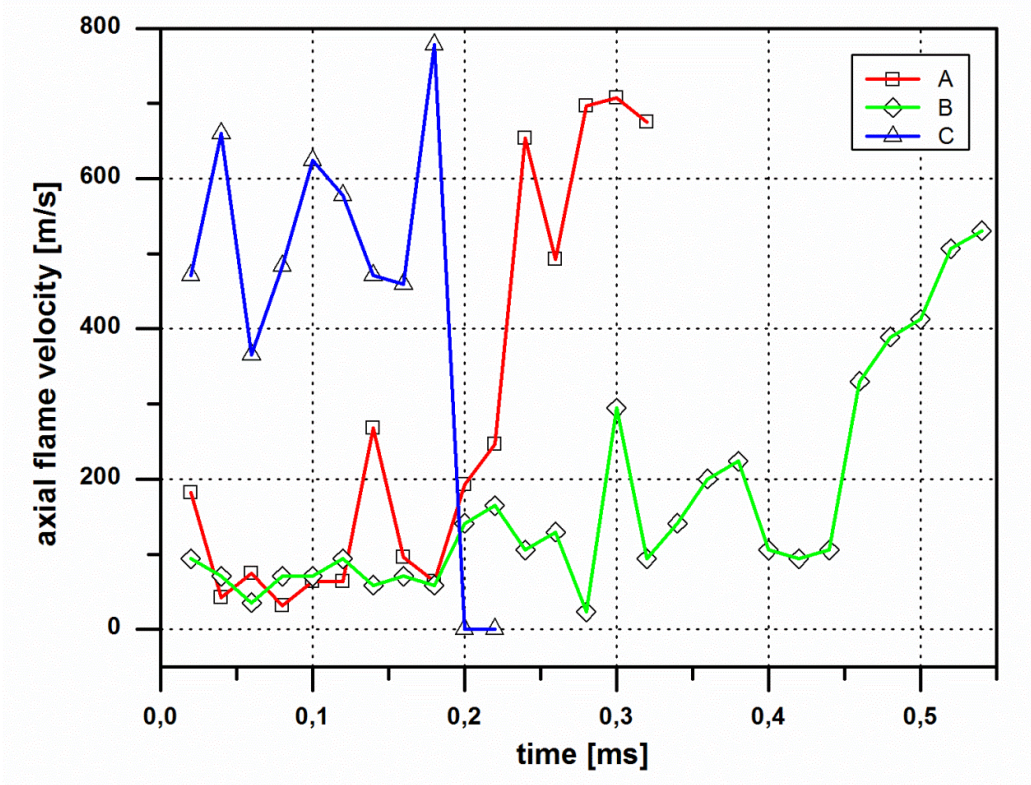

Numerical results
Species distribution

Test case	ROF	Mass fraction CH_4	Mass fraction O_2	Mass fraction N_2
A	21.8	0.043	0.936	0.020
B	19.2	0.035	0.677	0.288
C	2.2	0.194	0.426	0.379

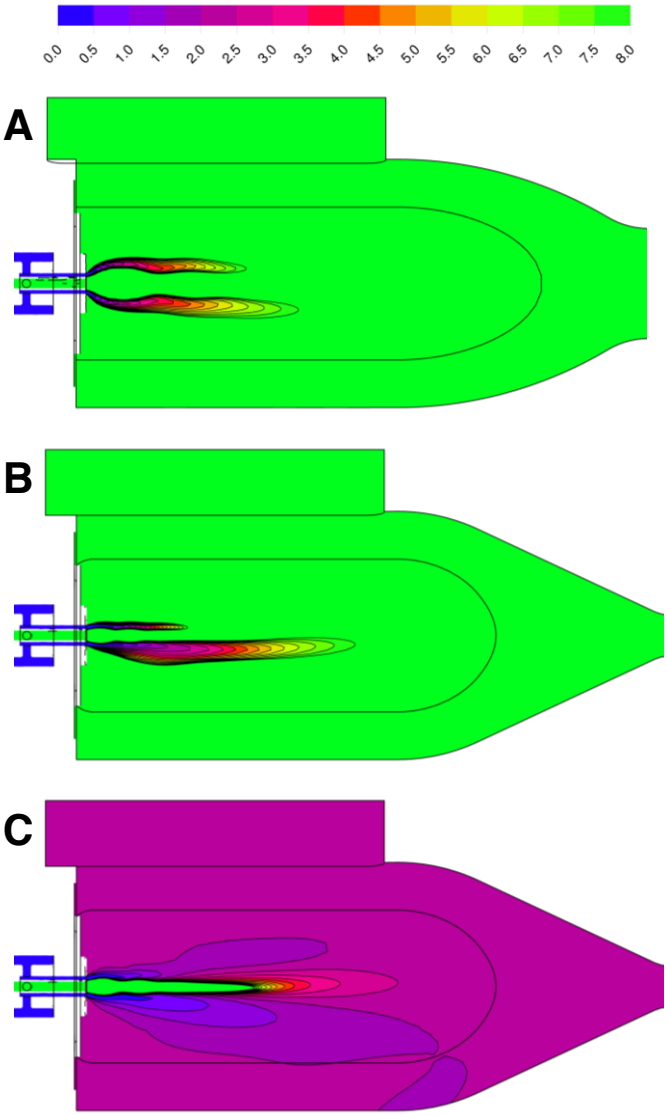

Results
Flame transition

A

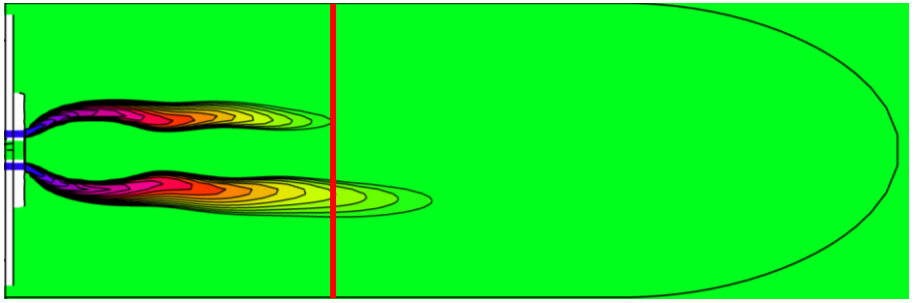

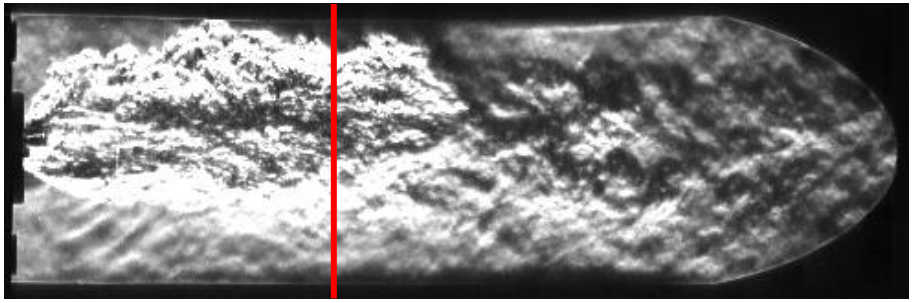

B

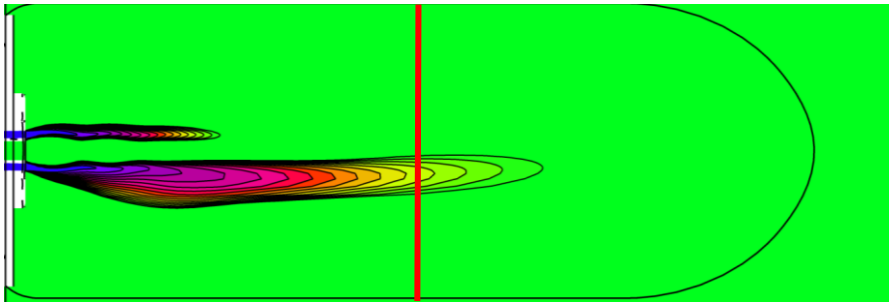

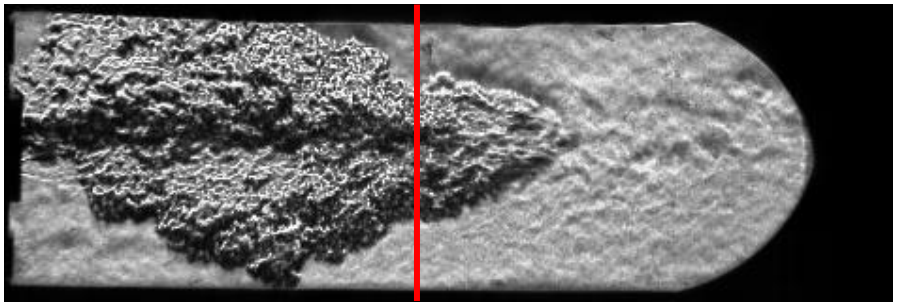

C

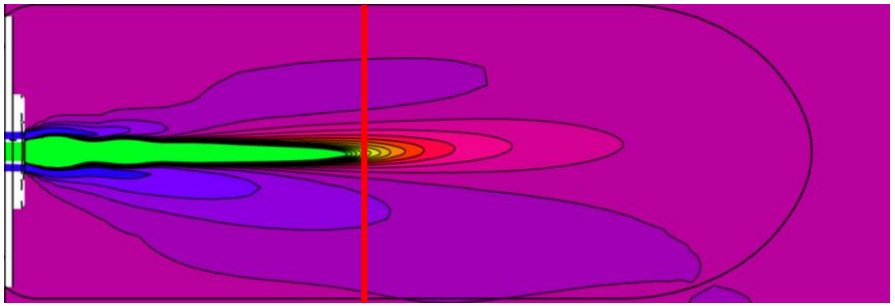

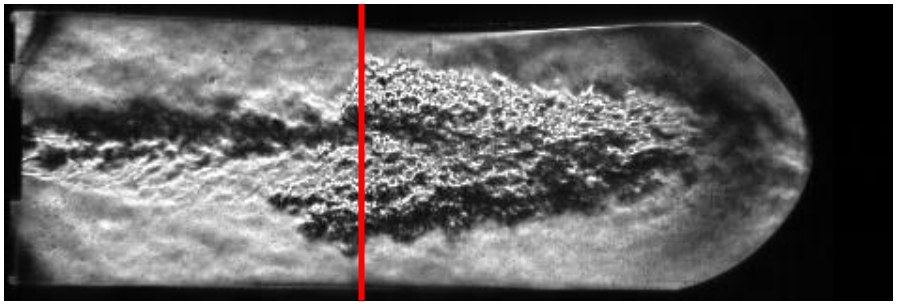

Summary

- Comparison of three laser ignition test cases with two different combustion chambers
- Experimental investigation of the flame development: flame front acceleration in hard ignition cases
- Numerical investigation of species distribution at the time of ignition: oxygen-rich environment causes hard ignition
- Transition of flame behaviour occurs when the flame reaches the well mixed propellant zones

- Fuel rich cold flow conditions and downstream ignition position are beneficial to achieve a smooth ignition

Thank you!

APPENDIX: Additional charts

Cold flow
Experiment vs. Simulation

10 ms

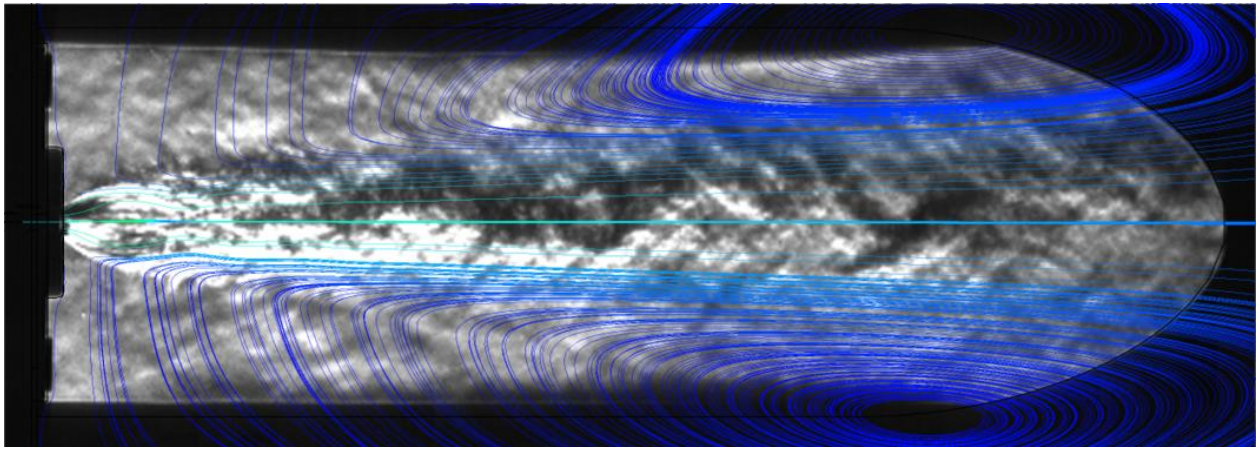

82 ms

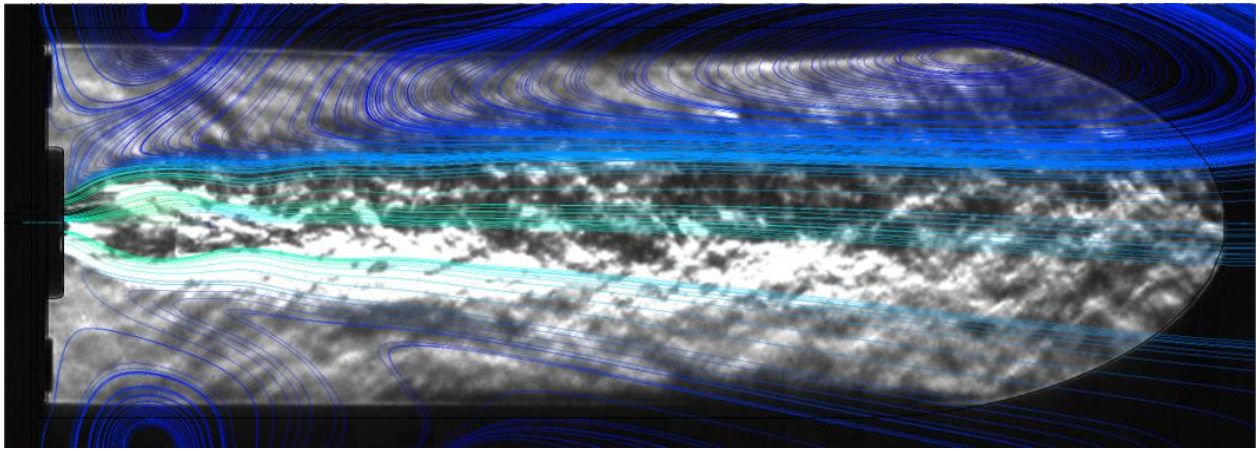

DLR

Results
Flame development

- Test cases A and B show flame acceleration
- Test case C shows opposite behaviour
- All three test cases show a transition of flame behaviour

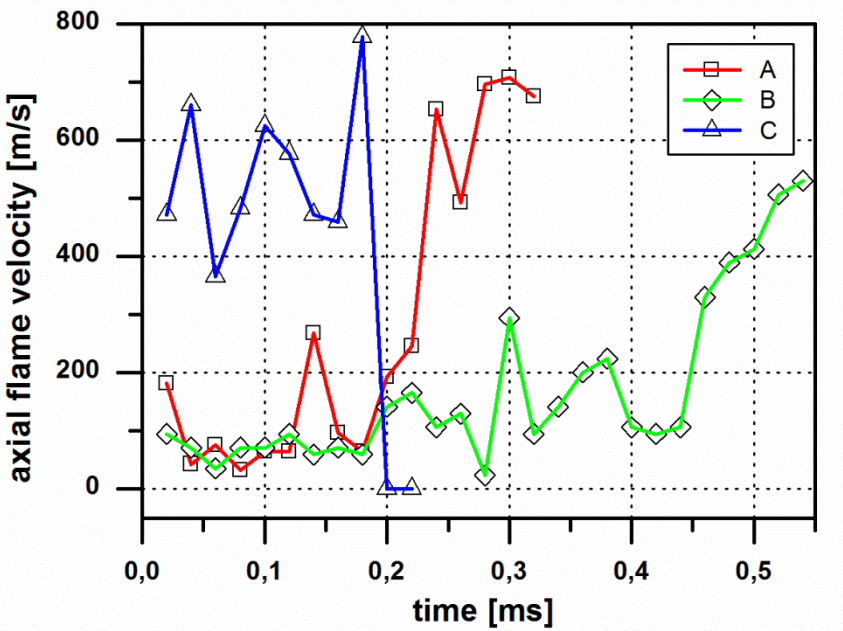

Results
Species distribution: ROF

- $ROF_{st} = 4$
- ROF-values clipped at ROF = 8
- Hard ignition cases: O_2-rich
  smooth ignition case: CH_4-rich

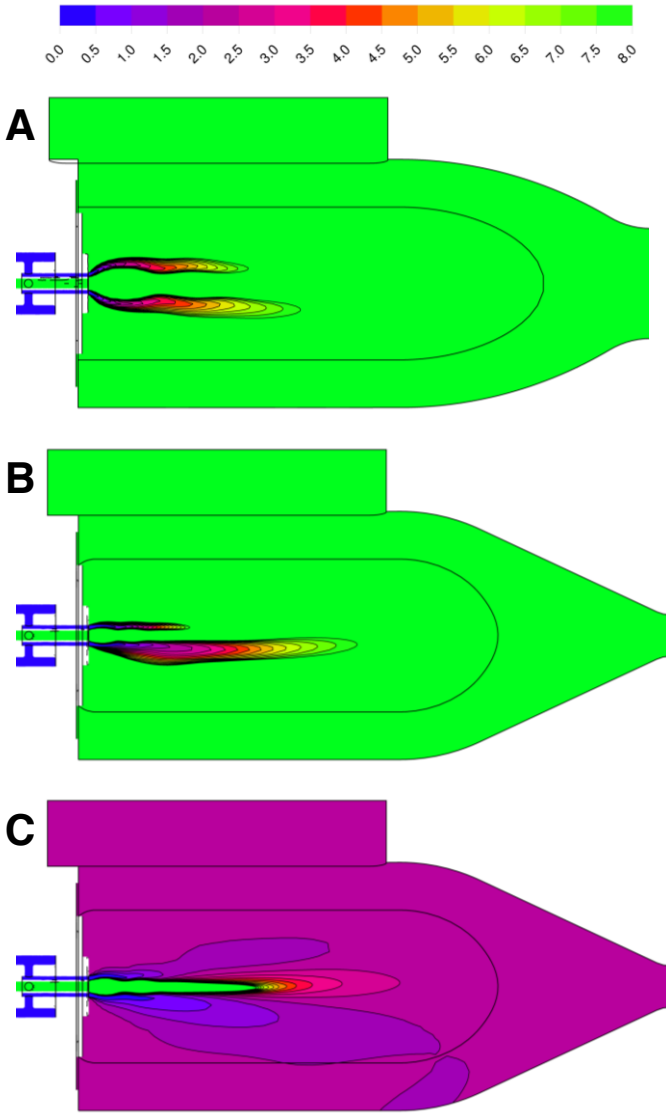

Numerical results
Species distribution

Test case	ROF	Mass fraction CH_4	Mass fraction O_2	Mass fraction N_2
A	21.8	0.043	0.936	0.020
B	19.2	0.035	0.677	0.288
C	2.2	0.194	0.426	0.379

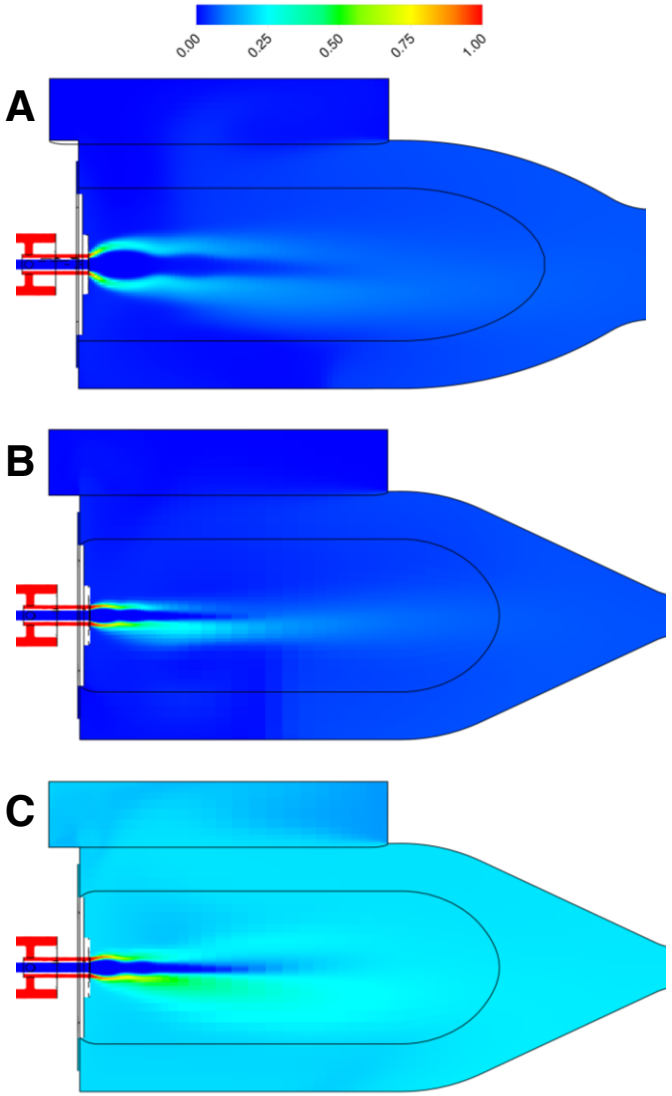

Results
Species distribution: CH_4

- Amounts of CH4 low in test cases A and B
- High amounts of CH4 in test case C

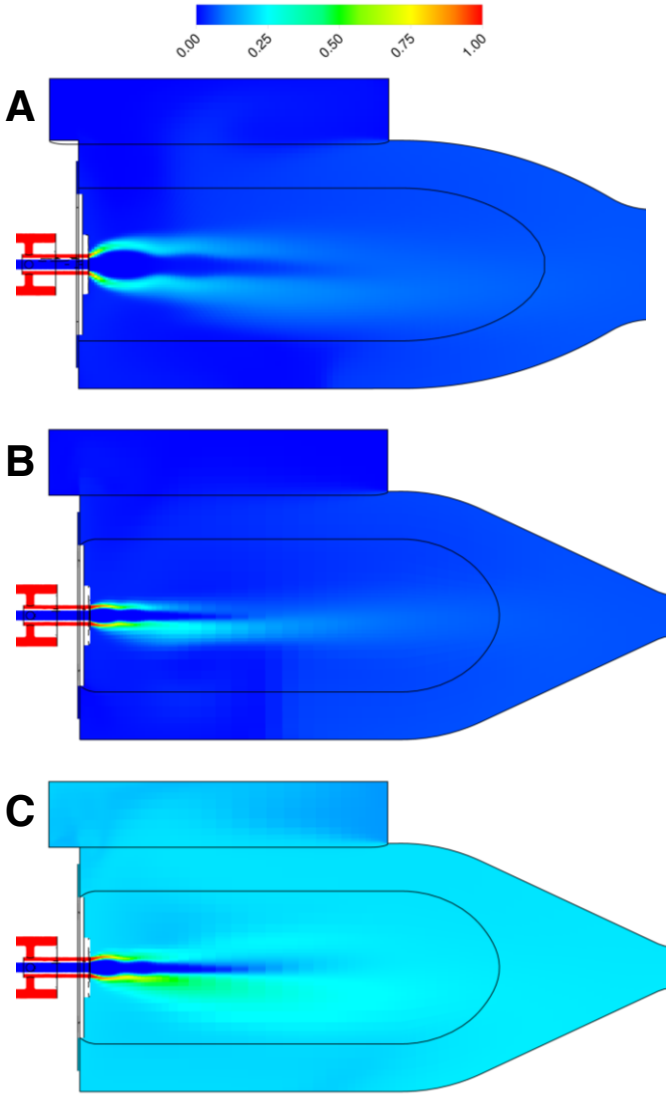

Numerical results
Species distribution

Test case	ROF	Mass fraction CH_4	Mass fraction O_2	Mass fraction N_2
A	21.8	0.043	0.936	0.020
B	19.2	0.035	0.677	0.288
C	2.2	0.194	0.426	0.379

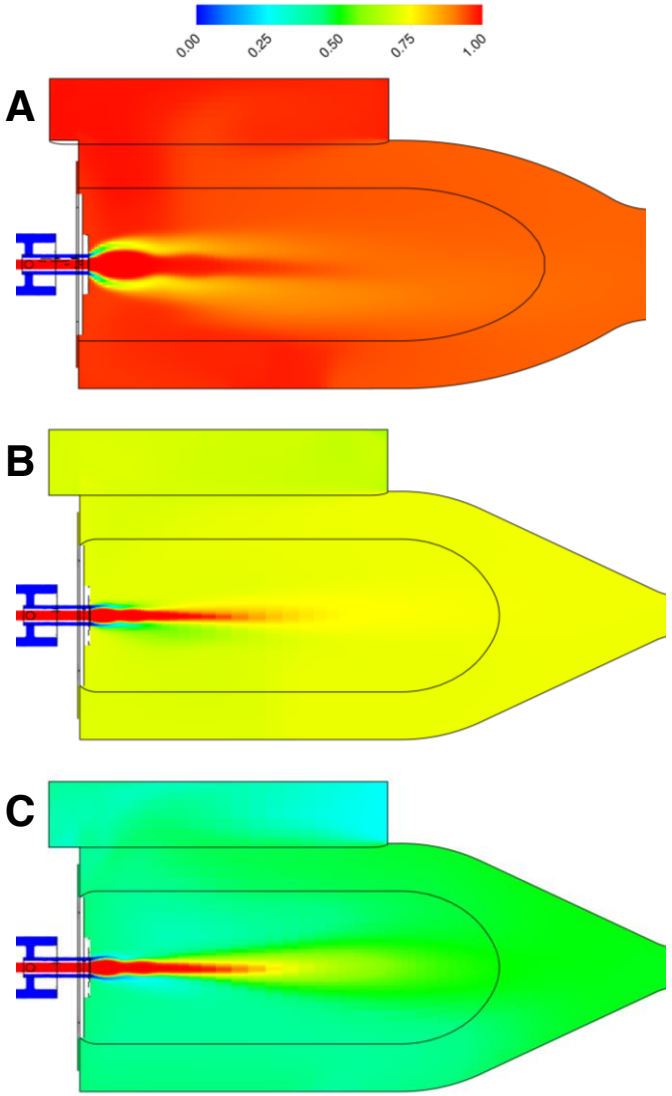

Results
Species distribution: O_2

- Test case A: Close to 100% O2 in large regions
- Test case B: ~75% O2 in recirculation zones
- Test case C: ~50% O2 in large regions

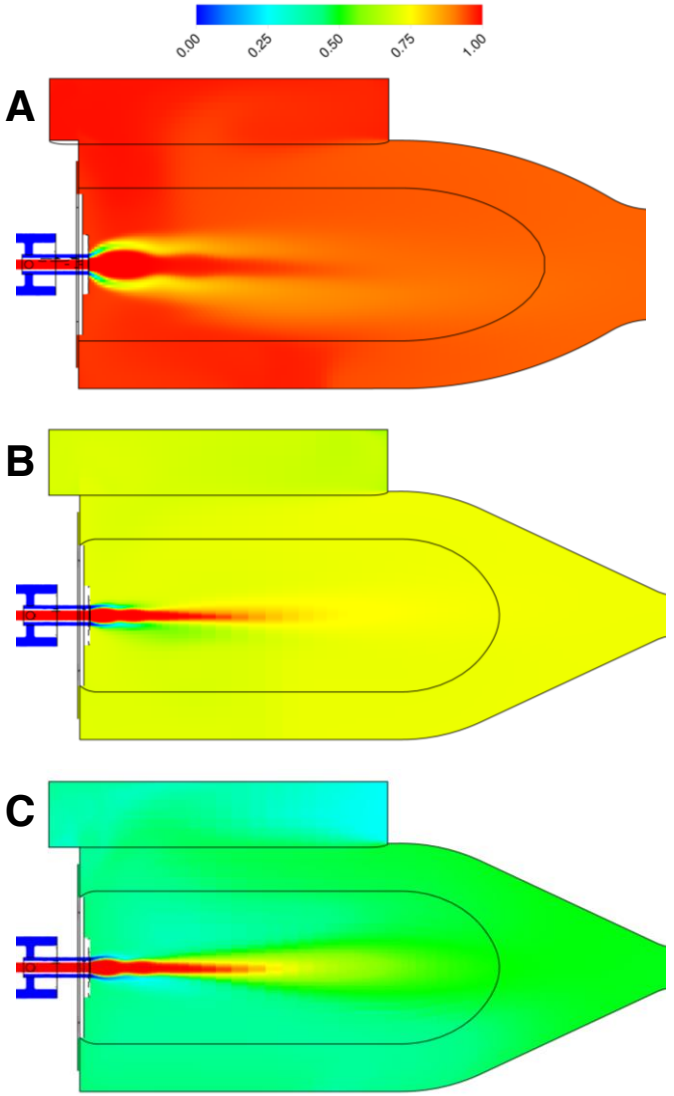

Numerical results
Species distribution

Test case	ROF	Mass fraction CH_4	Mass fraction O_2	Mass fraction N_2
A	21.8	0.043	0.936	0.020
B	19.2	0.035	0.677	0.288
C	2.2	0.194	0.426	0.379

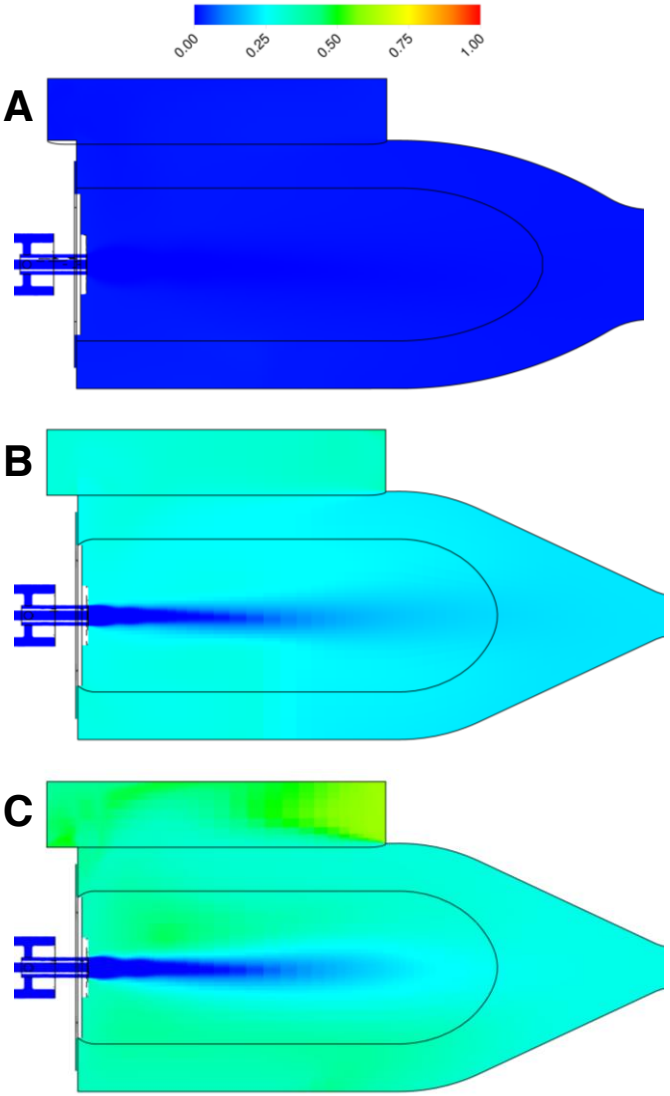

Results
Species distribution: N_2

- Test case A: almost no N_2 left
- Test case B: still residual N_2 in the chamber
- Test case C: highest amounts of N_2
- Comparison A and B: N_2 content has no significant impact on the flame development